



## Magnitude scaling relations from P-waves in southern California

Louisa L. H. Tsang,<sup>1,2</sup> Richard M. Allen,<sup>1</sup> and Gilead Wurman<sup>1</sup>

Received 21 June 2007; revised 10 August 2007; accepted 22 August 2007; published 5 October 2007.

[1] We derive empirical magnitude scaling relationships for southern California using a dataset of 59 past earthquakes recorded in southern California by the Southern California Seismic Network (SCSN) between 1992 and 2003. The events range in magnitude from 3.0 to 7.3. We use the maximum predominant period ( $\tau_p^{\max}$ ) and the peak displacement amplitude ( $P_d$ ) measured from the first 4 seconds of P-wave arrivals to determine period-magnitude and amplitude-magnitude scaling relationships respectively. Our calibration study shows that the scaling relationships are similar to those derived for northern California. The average error in magnitude estimates is 0.2 magnitude units for events with magnitudes smaller than 4.5 ( $M \leq 4.5$ ), 0.3 magnitude units for events with magnitudes ranging from 4.5 to 6.5 ( $4.5 < M \leq 6.5$ ), and 0.5 magnitude units for events with magnitudes greater than 6.5 ( $M > 6.5$ ). **Citation:** Tsang, L. L. H., R. M. Allen, and G. Wurman (2007), Magnitude scaling relations from P-waves in southern California, *Geophys. Res. Lett.*, *34*, L19304, doi:10.1029/2007GL031077.

### 1. Introduction

[2] The proximity of metropolitan cities to active faults within southern California presents a challenge in developing an earthquake early warning system (EEW) capable of providing advance warning of peak ground shaking associated with large earthquakes.

[3] Earthquake Alarm Systems (ElarmS) is a methodology to integrate realtime geophysical data during the course of an earthquake for the purpose of providing warnings prior to damaging ground shaking (<http://www.elarms.org/>). ElarmS uses multiple seismic stations to detect and locate earthquakes, estimate the magnitude from P-waves, and predict the distribution of ground shaking. The methodology was initially developed by Allen and Kanamori [2003], is described more fully by Allen [2007], and has been extended by Wurman *et al.* [2007]. ElarmS has been extensively tested offline within northern California, and shown effective as an algorithm for providing accurate estimates of earthquake magnitude, location and the distribution of peak ground acceleration within a few to a few tens of seconds after the earthquake origin time.

[4] Using the same methodology described by Wurman *et al.* [2007], we derive empirical magnitude scaling relationships exclusively for southern California and evaluate the quality of the calibration using 59 past earthquakes recorded

in the region. This provides the necessary scaling relations for future application of ElarmS to southern California. We also compare the magnitude scaling relationships derived in southern California with those derived for northern California.

### 2. Methodology

[5] The ElarmS methodology [Allen and Kanamori, 2003] was developed using past earthquake waveforms to derive empirical scaling relationships between the maximum predominant period ( $\tau_p^{\max}$ ) of the first 4 seconds of a P-wave arrival at a seismic station, and the final network-recorded event magnitude. A similar methodology is used in the UrEDAS system implemented in Japan [Nakamura, 1988].

[6] Wurman *et al.* [2007] improve upon the accuracy of produced magnitude estimates by incorporating an additional method for magnitude estimation: scaling the peak displacement or velocity amplitude ( $P_{d/v}$ ) of the first 4 seconds of a P-wave arrival with the final network-recorded magnitude via an empirically derived scaling relationship. [Wu *et al.*, 2006].

[7] In this study, we use a dataset of 59 past earthquakes to derive empirical best-fit period-magnitude and amplitude-magnitude scaling relationships for southern California. These events occurred in southern California between 1992 and 2003, and range in magnitude from 3.0 to 7.3. The dataset includes the three largest magnitude earthquakes for which digital recordings are available. The 1992 Landers event ( $M = 7.3$ ), the 1994 Northridge event ( $M = 6.7$ ) and the 1999 Hector Mine event ( $M = 7.1$ ). The waveforms were recorded by seismic stations within the Southern California Seismic Network (SCSN) and obtained from the Southern California Earthquake Center (SCEC). Figure 1 shows a map of all the events and SCSN stations used in this study.

[8] We plot observations of  $\tau_p^{\max}$  measured within the first 4 seconds of a P-wave arrival versus the network magnitude, and fit a least squares linear regression line to the observations. We define the period-magnitude scaling relationship as the equation of this line. Likewise, we obtain the amplitude-magnitude scaling relationship using observations of the peak displacement amplitude ( $P_d$ ) within the first 4 seconds of a P-wave arrival. We define the ElarmS magnitude estimate as the linear average of the magnitude estimates obtained from  $\tau_p^{\max}$  and  $P_d$ .

[9] Using the derived best-fit relationships and algorithmic components from ShakeMap specific to southern California [Newmark and Hall, 1982; Joyner and Boore, 1988; Boore *et al.*, 1997; Wald *et al.*, 1999, 2005], we run ElarmS on the 59 events in our dataset, and determine the associated magnitude errors and uncertainties in peak ground acceleration estimates at “alarm-time” (defined as the time when

<sup>1</sup>Department of Earth and Planetary Science, University of California, Berkeley, California, USA.

<sup>2</sup>Department of Earth Science and Engineering, Imperial College London, London, UK.

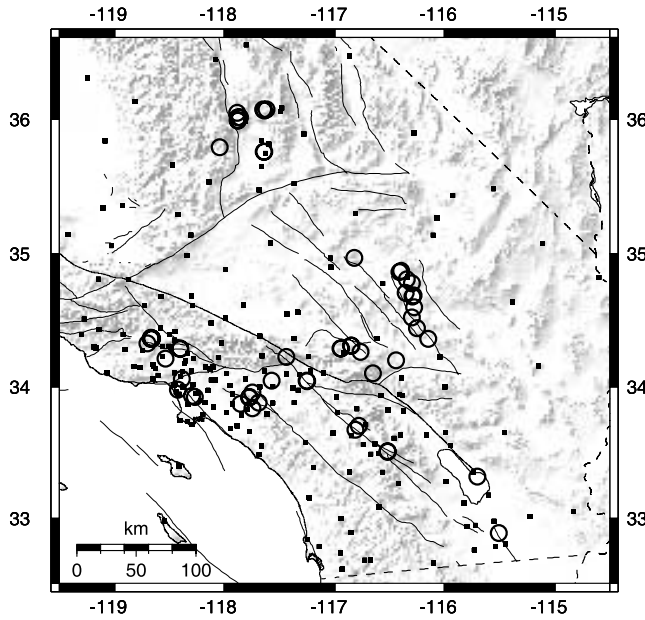


**Figure 1.** Map showing the location of the 59 earthquakes (circles) and Southern California Seismic Network (SCSN) stations (squares) used in this study.

4 seconds of data is available from 4 different channels), in order to evaluate the quality of the calibration.

### 3. Results

#### 3.1. Period-Magnitude Scaling Relationship

[10] We obtain the following best-fit relationship between  $\tau_p^{\max}$  in the first 4 seconds of a P-wave arrival at a station, and the event magnitude:

$$M = 6.36 + 6.83 \log_{10}(\tau_p^{\max}) \quad (1)$$

[11] The solid line in Figure 2a shows a plot of this relationship through the maximum predominant period observations from the 59 events used for the calibration. The variance of the observed  $\tau_p^{\max}$  values from the best-fit line is 0.0228 log units in period.

#### 3.2. Amplitude-Magnitude Scaling Relationship

[12] We obtain the following best-fit relationship between  $P_d$  in the first 4 seconds of a P-wave arrival at a station, and the event magnitude:

$$M = 1.24 \log_{10}(P_d) + 1.65 \log_{10}(R) + 5.07 \quad (2)$$

where  $R$  is the distance between the station and the epicenter, in kilometers. Here the variance between observed  $P_d$  and the model is 0.134 log units in amplitude. The solid line in Figure 2b shows a plot of this relationship through the peak displacement observations from the 59 events used for the calibration. Using this relation to estimate magnitude in a realtime early warning environment requires a good estimate of the epicentral distance and therefore the event location. This does not cause a problem when using the dense regional networks in California as

multiple stations have usually triggered by the time of the first magnitude estimate.

#### 3.3. Quality of the Calibration

[13] The average magnitude error using  $\tau_p^{\max}$  observations from a single seismic station is 1.1 magnitude units. This is greater than an average error of 0.4 magnitude units that we find using the peak displacement amplitude ( $P_d$ ) observations from a single station. Figure 3 shows a scatter plot of ElarmS magnitude versus network-recorded magnitude ( $M_w$  or  $M_L$ ). The dashed line on the plot represents a

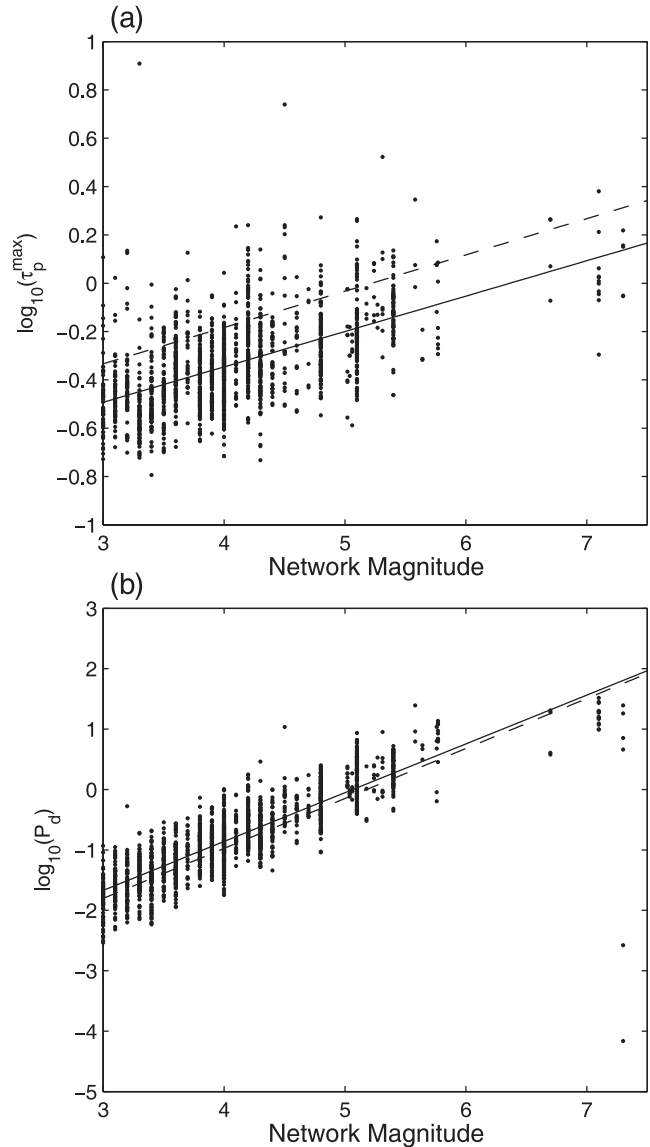


**Figure 2.** Plot of (a) maximum predominant period vs. network magnitude and (b) peak displacement amplitude vs. network magnitude for all 59 events (each peak value has been corrected to an epicentral distance of 1 km). Each point represents an individual station measurement using the first 4 seconds of a P-wave arrival. The solid line in each of the plots shows the best-fit linear scaling relation. The dashed line in each of the plots shows the respective scaling relationships derived for northern California [Wurman et al., 2007].

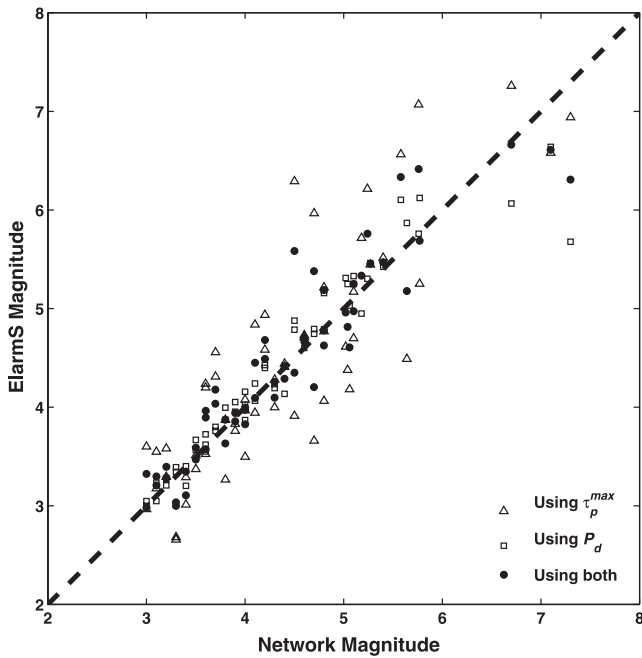


**Figure 3.** Plot of ElarmS magnitude estimate vs. network-recorded magnitude (in  $M_w$  or  $M_L$ ) for all 59 earthquakes. The triangles represent magnitude estimates using the maximum predominant period ( $\tau_p^{\max}$ ) observations, the squares represent the magnitude estimates using the peak displacement amplitude ( $P_d$ ), and the circles represent the magnitude estimates calculated by averaging magnitudes estimated using  $\tau_p^{\max}$  and  $P_d$ , for each earthquake.

1:1 relationship between the estimated magnitude and the observed magnitude. We can therefore evaluate the accuracy of the ElarmS magnitude calibrations by analyzing the scatter of the observation points about this line. The triangles plotted on Figure 3 show the magnitude estimates from  $\tau_p^{\max}$ . They show little scatter for small events ( $M < 4.5$ ), but more scatter for events with magnitudes greater than 4.5. The squares in Figure 3 represent the magnitude estimates from  $P_d$ . They lie remarkably close to the plotted dashed line when event magnitudes are smaller than 5.5. However, at magnitudes larger than 5.5, more scatter occurs. Joint  $\tau_p^{\max}$  and  $P_d$  magnitude estimates are plotted

as circles in Figure 3. The scatter in the combined ElarmS magnitude is significantly less than that of  $\tau_p^{\max}$  and  $P_d$  magnitude estimates individually, at a given network-recorded magnitude. This justifies using both estimators to provide the most accurate estimate of the earthquake magnitude.

[14] For small events (we define these as events with  $M \leq 4.5$ ), the average error in ElarmS magnitude estimates is 0.2 magnitude units. For moderate-sized events ( $4.5 < M \leq 6.5$ ), this error is slightly larger: 0.3 magnitude units. This is reflected by the greater scatter in Figure 3 at larger magnitudes. Since we are primarily concerned with the accuracy in parameter estimates of large earthquakes, which potentially cause the most socio-economic damage in cities, we evaluate the accuracy of the calibration for the three largest events in the dataset. In the case of the 1992 M7.3 Landers earthquake, the magnitude is underestimated by 1.0 magnitude units. The magnitude error is primarily due to the fact that there were only 2 stations to report  $\tau_p^{\max}$  and  $P_d$  measurements within 100 km of the epicenter at the time of earthquake. We find the ElarmS magnitude error for the 1999 M7.1 Hector Mine earthquake to be lower: 0.5 magnitude units. For the 1994 M6.7 Northridge earthquake, despite the fact that only 2 stations were located within 100 km of the epicenter, the magnitude is only underestimated by less than 0.1 magnitude units. The average ElarmS magnitude error for these three large events is 0.5 magnitude units.

[15] ElarmS provides realtime predictions of peak ground acceleration (PGA), peak ground velocity (PGV), and Modified Mercalli Intensity (MMI) using a similar approach to that used by ShakeMap. Here we present only the errors for PGA due to space limitations, however, they are representative of the errors in PGV and MMI also. Figure 4 shows the error in PGA estimates for all 59 events. This is expressed as the log (PGA) error, which is calculated by subtracting the logarithm of the observed peak ground acceleration from the logarithm of the estimated peak ground acceleration. An error of 1 represents an overprediction of the peak ground acceleration by a factor of 10. The plots in Figure 4 show that the log (PGA) error decreases from an average error of  $-0.5$  initially (i.e. 1 second after event detection) (Figure 4a) to 0.0 at “alarm-time” meaning that the PGA estimates are centered on the true value (Figure 4b). The standard deviation of the

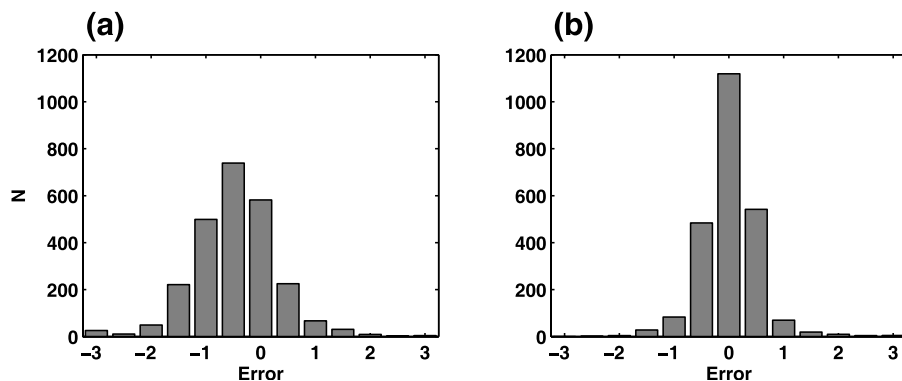


**Figure 4.** Histograms showing the error in peak ground acceleration (log (PGA) error) (a) initially (1 second after the first detected P-wave arrival) and (b) at “alarm-time”(time when 4 seconds of data is available from 4 different channels).

error in the log (PGA) estimates is 0.8 initially, and decreases to 0.5 at “alarm-time”. The log (PGA) errors associated with all three of the largest events at “alarm-time” were small. For the Northridge event, we find the average log (PGA) error to be  $-0.2$  with a standard deviation of 0.3 ( $-0.2 \pm 0.3$ ). This corresponds to an average underestimation of peak ground acceleration by a factor of 0.6. The log (PGA) errors for Landers and Hector Mine were less, ( $-0.1 \pm 0.2$ ) and ( $0.0 \pm 0.2$ ) respectively. It is worth noting that the PGA errors at “alarm-time” do not correlate with the size of the magnitude errors.

#### 4. Discussion

[16] Figure 2a shows that compared to northern California, shorter maximum predominant periods (higher frequencies) are found within southern California, for any given network magnitude. While the slight difference in scaling slope between northern and southern California is statistically insignificant with this dataset, the difference in scaling offset is a statistically significant result, with greater than 99.99% confidence (Student-t value of 7.17 with 1760 degrees of freedom). Presently we are unsure of reasons for this, although fault rupture dynamics and regional crustal structure may play a role in explaining this observation. For the amplitude-magnitude calibration, we find that measuring the peak amplitude in displacement ( $P_d$ ) yields the lowest errors for both velocity sensors and accelerometers. This therefore allows us to derive a single best-fit scaling relationship using  $P_d$  measurements only. By contrast, in northern California two individual amplitude-magnitude scaling relationships were necessary for velocity sensors and accelerometers; peak amplitude in displacement ( $P_d$ ) was used for velocity instruments, whereas peak amplitude in velocity records ( $P_v$ ) were used for accelerometers (for a full discussion to justify deriving scaling relationships for individual channels, refer to *Wurman et al.* [2007]). The lower errors associated with using peak amplitude in displacement in southern California may be attributed to the housing of accelerometers at stations located at lower noise sites. We speculate that the larger number of stations further from the coast in southern California are subject to less noise due to ocean waves and tides. Since we are able to obtain  $P_d$  measurements from both velocity sensors and accelerometers in southern California, we have a larger number of  $P_d$  data points on our scatter plot of  $P_d$  vs. network magnitude providing for a more robust fit. This ensures that we can obtain a well-constrained amplitude-magnitude scaling relationship. Figure 2b shows the similarity between the  $P_d$  amplitude-magnitude scaling relationships obtained for southern and northern California respectively.

[17] The dataset we use in this calibration study includes large magnitude events recorded by seismic networks when the density of station coverage was much lower than that of the present day. Hence the accuracy of rapid-magnitude estimates determined from ElarmS in this study would be further improved if we were able to include within our dataset large magnitude earthquake data recorded by a seismic network similar to today’s station coverage density. This study therefore exemplifies the threshold accuracy of magnitude and peak ground acceleration estimates ElarmS

can provide for large magnitude earthquake events. We calculate that if a repeat Hector Mine-sized earthquake occurs along the Lavic Lake/Bullion fault, ElarmS could potentially provide the following warning times for populated cities at “alarm-time”: 10 seconds for Barstow (located 75 kilometers from the epicenter); 20 seconds for Moreno Valley/Riverside (located approximately 104 kilometers away), and 30 seconds for downtown Los Angeles (located 190 kilometers away). The warning times given here indicate the amount of time available before the S-wave arrival, which is the earliest time at which peak ground shaking would occur. It should be noted that these times do not take into account delays due to transmission of data over seismic networks which would likely be a few seconds. The density of the seismic network in 1999 was similar to that of today, therefore these warning times are a good indication of the warning time ElarmS could provide.

#### 5. Conclusions

[18] The results of our calibration study show that the scaling relationships between  $\tau_p^{\max}$  and  $P_d$  measured from the first 4 seconds of the P-wave and earthquake magnitude are similar but not identical to those of northern California. Combining these scaling relations to determine the ElarmS magnitude estimate we find that the uncertainty for small magnitude events ( $M \leq 4.5$ ) is 0.2 magnitude units. For  $4.5 < M \leq 6.5$  events the uncertainty is 0.3 and for  $M > 6.5$  the uncertainty is 0.5. It is a challenge to estimate the accuracy for large events given the small waveform dataset available due to few events and fewer stations providing  $\tau_p^{\max}$  and  $P_d$  measurements at the time of the events. Errors in the peak ground acceleration estimates have a mean and standard deviation of ( $0.0 \pm 0.5$ ) at “alarm-time”. The errors for the three largest events were ( $-0.2 \pm 0.3$ ), ( $-0.1 \pm 0.2$ ) and ( $0.0 \pm 0.2$ ) for Northridge, Landers and Hector Mine respectively. The errors are smallest for the most recent Hector Mine earthquake by which time many more stations were operating in southern California. For this earthquake 11 channels were providing data about the earthquake at “alarm-time” while only 4 were available for both Northridge and Landers.

[19] Given the present day density of station coverage in southern California, these magnitude scaling relationships can potentially provide rapid and accurate real-time magnitude and ground motion estimates for populated areas in epicentral regions. This would allow existing seismic networks to provide seconds to tens of seconds warning prior to damaging ground shaking.

[20] **Acknowledgments.** The authors thank Pete Lombard for assistance in incorporating ShakeMap algorithms for southern California into ElarmS. This project was made possible by an exchange program between the Department of Earth Science and Engineering at Imperial College London, and the Department of Earth and Planetary Science at University of California Berkeley. Support for this work was provided by USGS/NEHRP grant 06HQAG0147.

#### References

- Allen, R. M. (2007), The ElarmS earthquake early warning methodology and its application across California, in *Earthquake Early Warning Systems*, edited by P. Gasparini, G. Manfredi, and J. Zschau, pp. 21–44, Springer, New York.
- Allen, R. M., and H. Kanamori (2003), The potential for earthquake early warning in southern California, *Science*, 300, 786–789.

- Boore, D. M., W. B. Joyner, and T. E. Fumal (1997), Equations for estimating horizontal response spectral and peak acceleration from western North American earthquakes: A summary of recent work, *Seismol. Res. Lett.*, *68*, 128–153.
- Joyner, W. B., and D. M. Boore (1988), Measurement, characterization and prediction of strong ground motions, in *Proceedings of the Conference on Earthquake Engineering and Soil Dynamics II, Geotech. Spec. Publ.*, vol. 20, pp. 43–102, Am. Soc. of Civ. Eng., Park City, Utah.
- Nakamura, Y. (1988), On the Urgent Earthquake Detection and Alarm System (UrEDAS), paper presented at Ninth World Conference on Earthquake Engineering, Int. Assoc. for Earthquake Eng., Tokyo, 2–9 Aug.
- Newmark, N. M., and W. J. Hall (1982), Earthquake spectra and design, *Geotechnique*, *25*, 139–160.
- Wald, D. J., V. Quitoriano, T. H. Heaton, H. Kanamori, C. W. Scrivner, and C. B. Worden (1999), TriNet ShakeMaps: Rapid generation of instrumental ground motion and intensity maps for earthquakes in southern California, *Earthquake Spectra*, *15*(3), 537–556.
- Wald, D. J., B. C. Warden, V. Quitoriano, and K. L. Pankow (2005), ShakeMap manual: Technical manual, user's guide and software guide, *Tech. Methods 12-A1*, U.S. Geol. Surv., Golden, Colo.
- Wu, Y.-M., H.-Y. Yen, L. Zhao, B.-S. Huang, and W.-T. Liang (2006), Magnitude determination using initial P waves: A single-station approach, *Geophys. Res. Lett.*, *33*, L05306, doi:10.1029/2005GL025395.
- Wurman, G., R. M. Allen, and P. Lombard (2007), Toward earthquake early warning in northern California, *J. Geophys. Res.*, *112*, B08311, doi:10.1029/2006JB004830.
- 
- R. M. Allen, L. L. H. Tsang, and G. Wurman, Department of Earth and Planetary Science, University of California, 307 McCone Hall, Berkeley, CA 94720-4767, USA. (rallen@berkeley.edu)